JOURNAL OF CATALYSIS 157, 396–402 (1995)

FTIR Study of CO/H_2 Reactions over Ru/TiO_2 and Ru–Rh/TiO_2 Catalysts at High Temperature and Pressure

Mandy W. McQuire and Colin H. Rochester

Department of Chemistry, The University, Dundee DD1 4HN, United Kingdom

Received January 23, 1995; revised June 13, 1995; accepted July 28, 1995

Infrared spectra are reported of Ru/TiO_2 and Ru–Rh/TiO_2 exposed to CO + H_2 at 553 K and 1.5 MN m^{-2} (15 atm). The Ru-Rh catalyst contained both exposed Ru and Rh atoms, which during reaction favoured adsorbed linear CO on Ru and bridged CO on Rh. Formation of an inactive long-chain hydrocarbon was accompanied by the appearance of a short-chain hydrocarbon which could be subsequently converted to methane. Ethoxide and ethanoate ions resulted from catalysis involving Rh. The results contrast with previous data for Ru–Rh/SiO_2. A 14:1 ratio of CO:H_2 over Ru–Rh/TiO_2 predominantly gave methane and an adsorbed CH_2-containing hydrocarbon. The mixed metal catalyst generated more methane but less surface hydrocarbon than either Ru/TiO_2 or Rh/TiO_2 catalysts.

INTRODUCTION

Titania as a support for Ru (1) and Rh (2) catalysts may lead to particularly high activities for CO hydrogenation reactions. Under high-temperature reduction conditions strong interactions between the metal and oxide catalyst occur (3) and may lead to decoration of the metal surface by TiO_x species (4–6). It has been proposed that sites at the junction between metal and TiO_x are highly active catalytically (4). However, there are reports that the activity of Ru/TiO_2 and Rh/TiO_2 catalysts are insensitive to reduction temperature (1, 6). An infrared study of Rh/TiO_2 exposed to CO + H_2 mixtures under high temperature and high pressure conditions has identified Rh carbonyl and Rh carbonyl hydride complexes which might be intermediates in specific catalytic reactions (7). Although Ru–Rh catalysts may be less active than Ru or Rh alone (8), the combined metals have been used in melt (9) or homogeneous (10) systems to prepare oxygenates from CO + H_2. Previous infrared studies of Rh/TiO_2 (7), Ru/SiO_2 (11), and Ru–Rh/SiO_2 (12) have therefore now been extended to the study of Ru/TiO_2 and Ru–Rh/TiO_2. Results for Ru–Rh/SiO_2 largely reflected the behaviour of Rh/SiO_2, suggesting that metal particles consisted of a core of Ru surrounded by a sheath of Rh.

EXPERIMENTAL

Degussa P25 titania (surface area 55 ± 1 m^2 g^{-1}, volume of pores <50 nm 0.11 ± 0.01 cm^3 g^{-1}, mean pore diameter 9.8 nm) was impregnated from aqueous solution with ruthenium nitrosyl nitrate (Johnson Matthey) alone or in a mixture with rhodium nitrate (Johnson Matthey) and dried in air at 383 K (16 h). A disc (100 mg, diameter 25 mm) was pressed (40 MN m^{-2}, 2 ton on die) and mounted in a steel infrared cell with fluorite windows before being reduced in a flow (0.1 MPa, 0.2 l min^{-1}) of 3.5% hydrogen in argon at 773 K (1 h), evacuated (773 K, $\frac{1}{2}$ h), and cooled to reaction temperature. Spectra of discs *in situ* at quoted high temperatures and high pressures of CO or CO + H_2 were recorded with a Perkin–Elmer 1750 FTIR spectrometer at 4 cm^{-1} resolution.

After reduction Ru/TiO_2 contained 2.5 wt.% Ru. Hydrogen and CO adsorption experiments gave H : Ru as 0.23 : 1 and CO : Ru as 0.38 : 1. The Ru–Rh/TiO_2 catalyst contained 1.25 wt.% Ru and 1.27 wt.% Rh, which gives equimolar proportions of Ru and Rh at a total loading that is equimolar to that for Ru alone in Ru/TiO_2. Hydrogen and CO uptakes gave H : (Ru + Rh) as 0.44 : 1 and CO : (Ru + Rh) as 0.42 : 1. The corresponding figures for a Rh/TiO_2 catalyst with a similar metal molar content (7) were 0.27 : 1 and 0.29 : 1, respectively, showing that the mixed system gave a better dispersion than either of the catalysts containing a single metal.

RESULTS

Ru/TiO_2

Spectra of Ru/TiO_2 exposed to CO at ambient temperature showed little change as the pressure was raised from 0.01 to 5 atm. Bands at 2040 and *ca.* 1970 (sh) cm^{-1} did not vary in either position or intensity with increasing pressure. However, some broadening of the dominant maximum due to linearly adsorbed CO on Ru^0 did occur. Direct addition of CO at high pressure to Ru/TiO_2 suggested that the broadening was partially caused by an additional band, present as a shoulder at ca. 1996 cm^{-1} and also attributable

0021-9517/95 $12.00

to CO linearly ligated to Ru. This shoulder remained for Ru/TiO_2 + CO at 673 K, by which temperature the main band was at 2022 cm^{-1}. At 573 K and above a weak sharp band at 1765 cm^{-1} increased in intensity with increasing temperature. A band at 1750 cm^{-1}, previously reported for CO on Ru/Al_2O_3 (13) and Ru/SiO_2 (11), has been ascribed to a μ-bonded carbonyl complex (13). The 2050–2200 cm^{-1} spectral region was obscured by intense maxima due to CO gas.

Study of the reactions of $CO:H_2$ mixtures over TiO_2 alone has been described in detail elsewhere (7). The infrared spectra of *in situ* reacting systems gave evidence, which was tested by the separate adsorption of MeOH, EtOH, HCOOH, and CH_3COOH, for the formation of methane gas and surface MeO^-, EtO^-, $HCOO^-$, and CH_3COO^- species and an adsorbed CH_2-containing hydrocarbon. However, the growth of hydrocarbon species for Ru/TiO_2 (Figs. 1b–1d) was initially considerably faster than the growth for TiO_2 alone under identical experimental conditions. Results emphasised here may be attributed to the presence of Ru in the catalyst. This does not preclude the possibility of synergistic catalysis involving both Ru and TiO_2 or spillover onto TiO_2 of products formed by catalysis on Ru.

Exposure of Ru/TiO_2 at 553 K to a 1:2 ratio of $CO:H_2$ at a total pressure of 1.5 MN m^{-2} gave infrared bands at 2040 and 1966 cm^{-1} due to surface carbonyl complexes of ruthenium. As the reaction proceeded, the former band shifted to 1971 cm^{-1} and became weak and the band at 1966 cm^{-} apparently disappeared. Gas-phase CO was progressively depleted. Carbon dioxide (band at 2350 cm^{-1}) was formed over the first 4.5-h reaction but then it too was depleted. Negligible water was formed as indicated by the absence of a band at 1620 cm^{-1} due to water adsorbed on the titania support. The fastest growth of bands due to hydrocarbon species occurred initially at 2960, 2919, and 2850 cm^{-1} (Figs. 1b–1d). However, with increasing time these bands due to vibrations of CH_3 and CH_2 groups in adsorbed linear hydrocarbons decreased in intensity and the spectrum in the CH-stretching region became dominated by a sharp maximum at 3016 cm^{-1} together with the *P* and *R* branch fine structure associated with methane gas (Figs. 1e and 1f). Removal of methane by evacuation left maxima at 2919 and 2850 cm^{-1}, suggesting (7, 14) that residual methylene-containing species remained (Fig. 1g). The band at 2919 cm^{-1} may also contain a contribution due to adsorbed CH_3 groups on the Ru catalyst component (15). The lower spectral region (1200–1600 cm^{-1}) only exhibited bands due to methane (1305 cm^{-1}) and CH_2 groups in methylene chains in accordance with the ν_{CH} data. Results in the latter region for Ru/SiO_2 under identical experimental conditions (11) are shown in Figs. 1h and 1i for comparison with the spectra for Ru/TiO_2.

Reaction of a 14:1 ratio of $CO:H_2$ over Ru/SiO_2 gave no methane and only an adsorbed long-chain hydrocarbon as product (11). Figure 2 for the corresponding reaction over Ru/TiO_2 also showed only slight evidence for methane (3016 cm^{-1}), the spectra being dominated by bands at 2933 and 2833 cm^{-1} initially (Fig. 2b), giving way to more intense bands at 2960, 2919, and 2850 cm^{-1} (Figs. 2f–2h). The two most intense bands at 2919 and 2850 cm^{-1} may again be ascribed to CH_2 groups with a possible contribution from CH_3 (ads). Comparison of the overall shapes in Figs. 1 and 2 for the band envelopes due to adsorbed species shows that different types or chain lengths of CH_2-containing alkyl groups must be contributing to the spectra. A significant band at 2960 cm^{-1} (Figs. 1b and 2h) due to a $\nu(CH_3)$ vibration in CH_3CH_2 groups contrasts with only a weak $\nu(CH_3)$ band in some spectra (Fig. 2g). The relative intensities of the bands at 2919 and 2850 cm^{-1} also differ appreciably in Figs. 1 and 2.

Possible bands at 2000–2200 cm^{-1} due to CO ligated to Ru in spectra of $CO:H_2$ and Ru/TiO_2 with a CO pressure of 1.4 MN m^{-2} were completely obscured by intense maxima due to CO gas (7). Attempts to reveal the bands by spectral subtraction and reducing the path-length in the infrared cell with fluorite space fillers were unsuccessful.

Ru–Rh/TiO_2

Spectra of Ru–Rh/TiO_2 in CO at high pressure gave a band at ca. 2040 cm^{-1}, the position of which hardly varied with increasing temperature. The spectra were more reminiscent of the results for Ru/TiO_2 than for Rh/TiO_2 (7). However, weak maxima at ca. 1920 cm^{-1}, shifting to 1900 with increasing temperature, 1836 cm^{-1}, shifting to 1850 cm^{-1}, and 1830 cm^{-1} were all typical in position and behaviour of Rh/TiO_2 rather than Ru/TiO_2, the bands being attributable to bridging carbonyl complexes of rhodium. In contrast a sharp band at 1765 cm^{-1} appearing at high temperatures resembled a similar band for Ru/TiO_2. The results imply that both exposed Rh and Ru surface sites are available for adsorption of CO in the temperature range 293–623 K. Spectra of Ru–Rh/TiO_2 in CO at 293 K showed no significant change in the pressure range 0.001–0.5 MN m^{-2}.

A 1:2 ratio of $CO:H_2$ admitted to Ru–Rh/TiO_2 at 553 K gave bands at 2080, 1973 (sh), 1855, and 1739 cm^{-1} due to metal carbonyl complexes (Fig. 3a). After considerable reaction, bands at 2170 and 2120 cm^{-1} due to CO (g) had diminished in intensity and surface metal carbonyls gave two dominant maxima at 2022 and 1858 cm^{-1} (Fig. 3g). Carbon dioxide (2350 cm^{-1}) was formed. Adsorbed hydrocarbon appeared in the system before methane (Fig. 3b) but eventually the band due to methane attained the largest maximum absorbance (Fig. 3g). Evacuation at 553 K removed methane and revealed bands at 2954, 2916, 2877, and 2848 cm^{-1} (Fig. 4c), which differed appreciably from

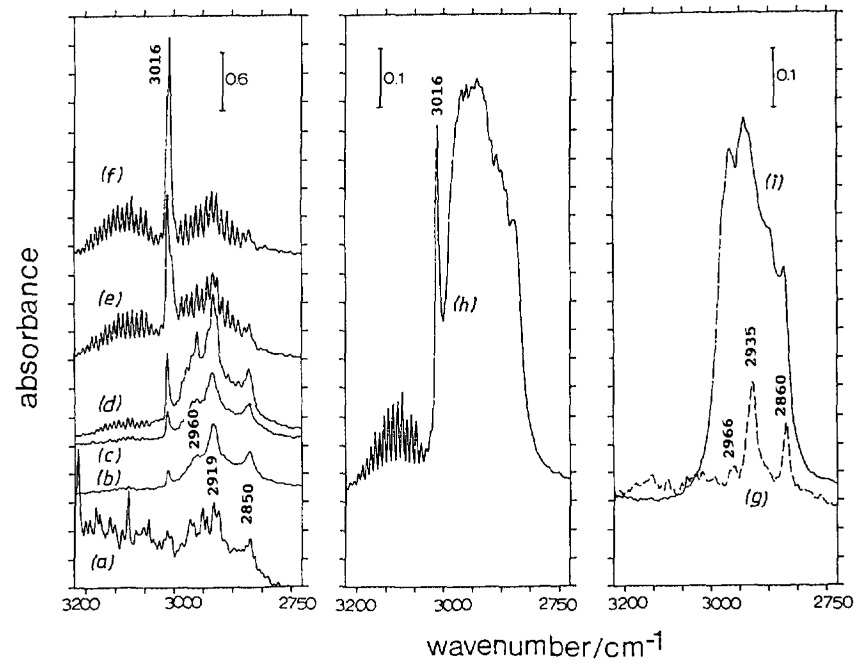

FIG. 1. Spectra of Ru/TiO_2 exposed at 553 K to CO (0.5 MN m^{-2})/H_2 (1.0 MN m^{-2}) for (a) ca. 1 min and (b) ½, (c) 1, (d) 2, (e) 5, and (f) 20 h, followed by (g) evacuation at 553 K (10 min). (h) Spectrum of Ru/SiO_2 after 70 h under the same conditions, followed by (i) evacuation at 553 K.

the bands for $Ru-Rh/SiO_2$ after reaction under the same conditions (Fig. 4d). Strong residual bands at 1525 and 1446 cm^{-1} (Fig. 3h) were primarily due to vibrations of ethanoate anions on the titania support (7, 16, 17). Raising the sample temperature to 723 K during evacuation failed to remove any hydrocarbon or ethanoate species from the catalyst surface.

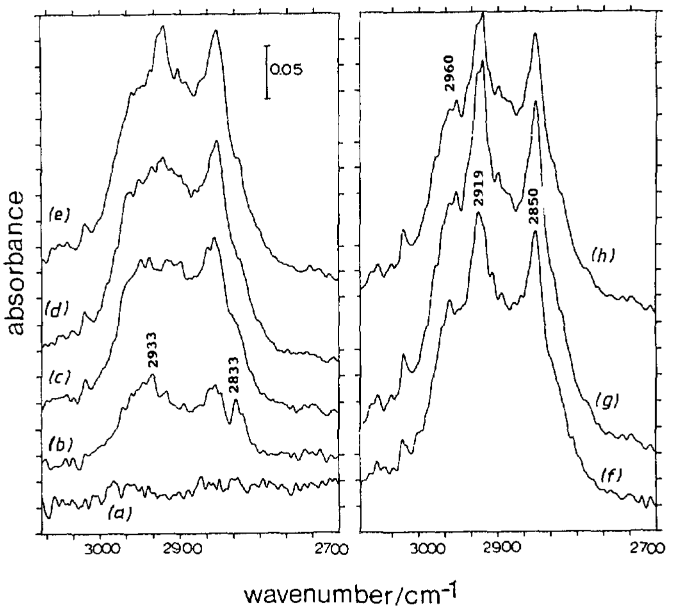

FIG. 2. Spectra of Ru/TiO_2 exposed at 553 K to CO (1.4 MN m^{-2})/H_2 (0.1 MN m^{-2}) for (a) 0, (b) *ca.* 1 min and (c) 1, (d) 5, (e) 10, (f) 30, (g) 40, and (h) 45 h.

Spectra of $Ru-Rh-TiO_2$ in a 14:1 ratio of $CO:H_2$ at 553 K exhibited the growth of a strong band due to CO_2 and weaker bands due to methane and adsorbed hydrocarbon (Fig. 5). Evacuation revealed that the dominant hydrocarbon adsorbed on the catalyst consisted primarily of CH_2 groups giving infrared bands at 2917 and 2850 cm^{-1} (Fig. 5c). The 1700–2200 cm^{-1} region of the spectrum was dominated by intense bands due to CO (g). A shoulder at ca. 2060–2070 cm^{-1}, disappearing with time, was possibly discernible but there was zero evidence for bridged metal carbonyls.

DISCUSSION

Results for CO adsorption on the present catalyst may be compared with results for Ru–Rh supported on SiO_2 (12). A metal surface containing both Ru and Rh adsorption sites for the TiO_2 support contrasted with the result for SiO_2, where metal particles consisted of a core of Ru with a, possibly monatomic, sheath of Rh. Dispersion values based on hydrogen chemisorption (100 H/metal atoms) were 48% for $Ru-Rh/SiO_2$ (12), which lay between values of 75% and 37% for Rh/SiO_2 (17) and Ru/SiO_2 (11), respectively, and 44% for $Ru-Rh/TiO_2$, which was higher than both the values, 29% and 23%, for Rh/TiO_2 (7) and Ru/TiO_2, respectively. The nature of the support therefore has a significant influence on the structure of the resulting

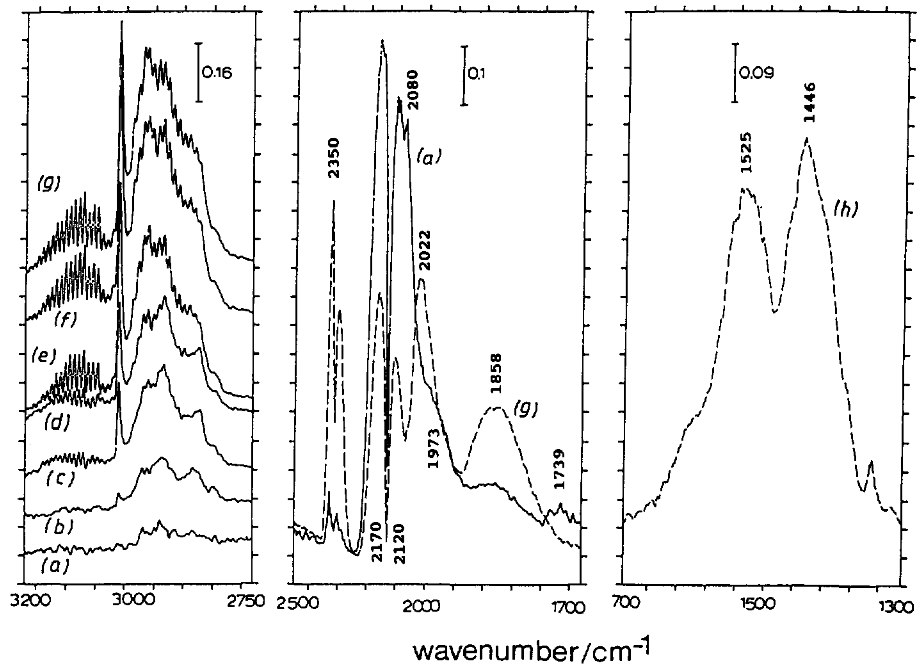

FIG. 3. Spectra of Ru–Rh/TiO_2 exposed at 553 K to CO (0.5 MN m^{-2})/H_2 (1.0 MN m^{-2}) for (a) *ca.* 1 min and (b) 1, (c) 10, (d) 20, (e) 50, (f) 70, and (g) 90 h, and (h) after subsequent evacuation at 553 K.

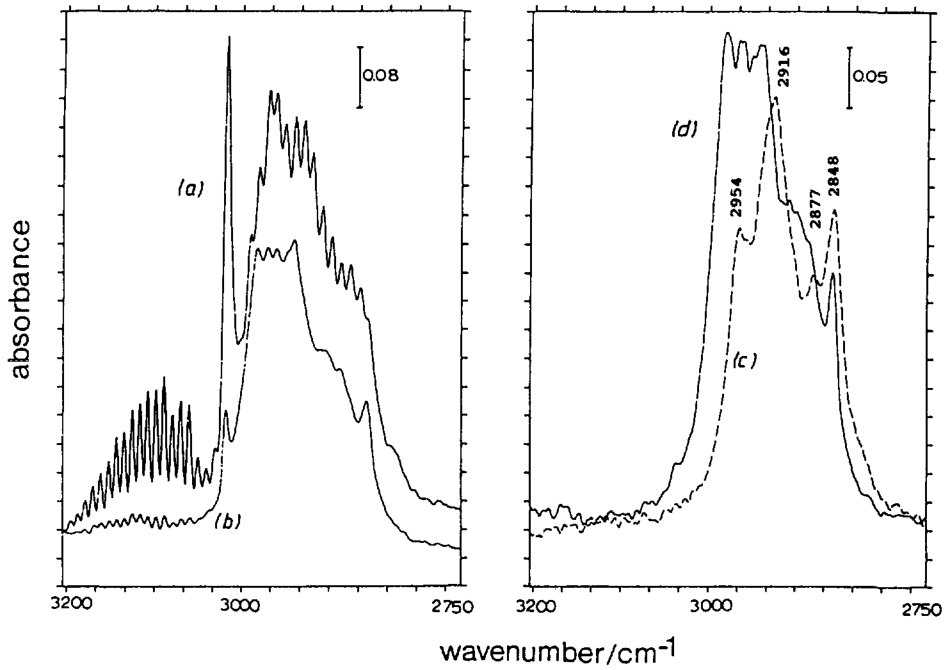

FIG. 4. Spectra of (a) Ru–Rh/TiO_2, (b) Ru–Rh/SiO_2 at 553 K after 90 h exposure to CO (0.5 MN m^{-2})/H_2 (1.0 MN m^{-2}), and after subsequent evacuation at 553 K for (c) Ru–Rh/TiO_2 and (d) Ru–Rh/SiO_2.

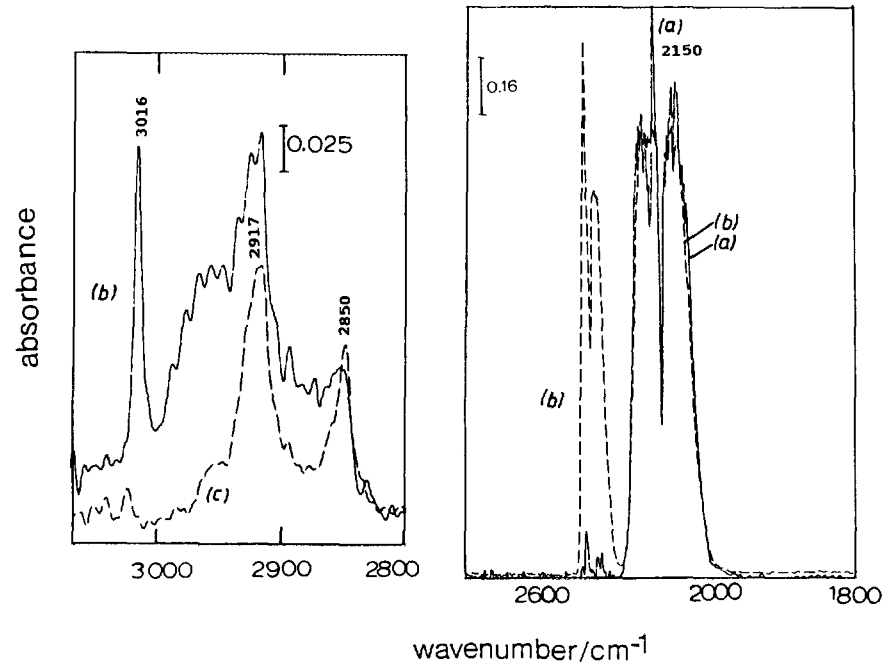

FIG. 5. Spectra of Ru–Rh/TiO$_2$ at 553 K exposed to CO (1.4 MN m^{-2})/H$_2$ (0.1 MN m^{-2}) for (a) *ca.* 1 min, (b) 70 h, and (c) after evacuation at 553 K.

Ru–Rh metal dispersion at least under the present preparative conditions, which were identical for all the catalysts (7, 11, 12, 18). Titania favoured high dispersion in the mixed system with exposed Ru and Rh surface sites.

It was not possible to deduce whether the Ru and Rh atoms in Ru–Rh/TiO$_2$ were exposed in a common surface or were partially segregated in patches on particle surfaces. However, bands due to bridging Rh carbonyls were at 1920 and 1836 cm^{-1} at ambient temperature, changing to 1900, 1850, and 1832 cm^{-1} at higher temperatures, which compare with band positions of 1918 and 1850 cm^{-1} shifting to 1900, 1850, and 1832 cm^{-1} for Rh/TiO$_2$ in the absence of Ru (7). Similarly a band at 1756 cm^{-1} was present in spectra of both Ru–Rh/TiO$_2$ and Ru/TiO$_2$. These results suggest that either segregation of Ru and Rh occurred in exposed surfaces and each behaved as if it alone existed in the system or the influences of adjacent heterometal atoms on each other were insufficient to change ν(CO) for bridge-bonded CO. For the mixed system there were no new infrared bands which could be ascribed to CO bridged across Ru and Rh atoms simultaneously.

Results for Rh/TiO$_2$ (7) and Ru/TiO$_2$ in the 1950–2100 cm^{-1} spectral region overlapped too much for a detailed analysis to be carried out for the mixed system. However, in general, spectra of Ru–Rh/TiO$_2$ in CO + H$_2$ mixtures exhibited bands ascribable to adsorbed CO interacting with both Rh (2080, 1855 cm^{-1}) and Ru (1973, 1739 cm^{-1}) sites. The shift to lower wavenumbers in the position of the band due to linearly adsorbed CO (Fig. 3g) with time resembles results for both supported Rh (7, 18) and Ru (11, 19) and for Ru–Rh/SiO$_2$ (12). However, the final band position at 2022 cm^{-1} is more typical of the results for Ru (20) rather than Rh, suggesting that the stationary state conditions for the reacting systems primarily involved linearly adsorbed CO at Ru surface sites. In contrast, the growth of the strong band at 1858 cm^{-1} with time is characteristic of an enhancement in bridge-bonded CO on Rh (7, 18). Factors affecting infrared band intensities and positions for linearly adsorbed CO include coadsorption of hydrogen (21–24), coadsorption of oxygen (19), structural reorganisation (22, 25–27), or carbon laydown resulting from dissociative adsorption of CO (22, 28–30).

Results for Rh/TiO$_2$ (7) suggested that carbon deposition and structural reorganisation of Rh to give sites favouring bridged CO might be linked. A corollary compatible with the present data would be that promotion of the formation of carbonaceous (28–30) and hydrocarbonaceous (19) deposits by Ru has an influence on metal aggregates, leading to Ru favouring linearly adsorbed CO, which has been proposed as the active precursor of CO hydrogenation over Ru (31), and Rh, which favours bridge-bonded CO adsorption. This effect was not observed for Ru–Rh/SiO$_2$ catalyst under identical experimental conditions (12) because in the absence of exposed Ru the catalyst, even after prolonged exposure to CO + H$_2$, exhibited surface properties typical of Rh alone.

The dissociative adsorption of CO as a precursor of surface carbon or hydrocarbon also leads to O-adatoms which may be a precursor of CO_2 (g) (29), which was a reaction product here (Fig. 3). Gupta *et al.* (20) studied $CO_2 + H_2$ reactions over Ru/TiO_2 and concluded that an infrared band at *ca.* 2020 cm^{-1} could be ascribed to a RuO(CO) species in which an O-adatom and a CO molecule were simultaneously ligated to a single Ru site. This attribution is unlikely to be valid for the present Ru–CO band at 2022 cm^{-1} since it is more reasonable to expect that a RuO(CO) species would give a band at a significantly higher wavenumber because of Ru cationic character induced by an O-adatom. Also the exact band position for CO linearly adsorbed on Ru^0 is particularly sensitive to the intermolecular interactions with neighbouring adsorbate molecules and with the dimensions of Ru^0 adsorption patches (23) and can appear anywhere within the range 1990–2060 cm^{-1}.

Titania alone catalysed the formation of methane and surface alkyl species from CO/H_2 mixtures (7). However, this was insufficient to account for the much faster formation of methane and surface hydrocarbon (which gave a spectrum (Fig. 1d) different from that for TiO_2 alone) over Ru/TiO_2 rather than Ru/SiO_2 (11). Whereas hydrocarbon on Ru/SiO_2 was maintained after build-up at a stationary steady state level, the initially more rapidly developed hydrocarbon on Ru/TiO_2 became depleted with time, suggesting its desorption (perhaps induced by carbon laydown or structural reorganisation of Ru) or further reaction. Infrared studies of Ru/Al_2O_3 and Ru/SiO_2 catalysts have identified surface hydrocarbon species which undergo hydrogenation (11, 19, 32, 33), possibly giving methane (34). Two types of surface hydrocarbon have been reported for Ru/SiO_2 (11, 19), one of which may involve direct interactions between each constituent CH_2 group and the metal surface and the other involves linear methylene chains only interacting at one or both ends with the surface. The former species was reactive towards hydrogenation but the latter was not. The reactive, or disappearing (Figs. 1d and 1e), species here contained a significant terminal methyl (19, 33) component (2960 cm^{-1}) and was therefore a short-chain species on the catalyst surface. The unreactive species exhibited dominant bands due to CH_2 groups (Fig. 1g) and was therefore a long-chain hydrocarbon (33). The specific difference between Ru/TiO_2 and Ru/SiO_2 catalysts may arise because of the enhanced activity of Ru–titania junction sites in Ru/TiO_2 although there is one report which suggests that this is unlikely (6). Alternatively the catalytic activity of TiO_2 alone for methane production (7) may be considerably enhanced by spillover of both hydrocarbon and activated H-adatoms (35) from the metallic Ru catalyst component to the surface of the TiO_2 component (either TiO_2 particles or TiO_x decoration on the metal).

The rate of appearance of the IR band at 3016 cm^{-1} due to methane over Ru–Rh/TiO_2 (Fig. 4a) was much less than the corresponding rates for Ru/TiO_2 (Fig. 1f) or Rh/TiO_2 (36) under identical preparative and reaction conditions. Dispersions were 44%, 23%, and 29%, respectively, and therefore it is unlikely that the Ru–Rh catalyst contained completely separate Ru and Rh particles (unless larger particles are more active per exposed metal atom). The result may be attributed to an ensemble effect (8) involving exposed Ru and Rh atoms in common surface planes. The infrared spectrum of adsorbed hydrocarbon (Fig. 4c) confirms that both Ru and Rh atoms exist in the catalyst surface because of the presence of bands characteristic of hydrocarbon and ethoxide anions (7) derived from catalysis over Ru and Rh, respectively. The strong bands at 1525 and 1446 cm^{-1} attributed to bidentate chelating ethanoate anions on the TiO_2 support (16, 17) are also a product of catalysis involving Rh (7) and not Ru. In contrast, Ru–Rh/SiO_2 gave results identical to those for Rh/SiO_2 with no evidence for catalysis by the Ru component (12).

The build-up of surface hydrocarbon for Ru–Rh/TiO_2 continued without depletion for long contact times (Fig. 3). This contrasted with the result for Ru/TiO_2 (Fig. 1). Again this may be an ensemble effect, the hydrogenation of surface hydrocarbon requiring a particular minimum grouping of exposed Ru atoms. Also Ru is much more reactive than Rh for methane formation at least when supported on Al_2O_3 (34).

Surface hydrocarbon formed from a CO-rich 14:1 mixture of CO:H_2 over Ru–Rh/TiO_2 at 553 K (Fig. 5) resembled similar species formed under the same experimental conditions over Ru/TiO_2 (Fig. 1), Rh/TiO_2 (7), and Ru–Rh/SiO_2 (12). Band intensities showed that the relative rates of growth of surface hydrocarbon were, in terms of catalyst, Rh/TiO_2 > Ru/TiO_2 > Ru–Rh/TiO_2. Furthermore, and in contrast to the results for the 1:2 ratio of CO:H_2, the ability of the catalysts to generate methane was in the sequence Ru–Rh/$TiO_2 \geq$ Ru/$TiO_2 \gg$ Rh/TiO_2. An Ru–Rh/SiO_2 catalyst produced negligible methane under the same conditions (36). A plausible link might be that less surface hydrocarbon is paralleled by less surface carbon (30) and hence (37) by a faster methanation rate. The generation of surface carbon may be accompanied by the concomitant formation of CO_2 (g) for which there is strong evidence (2350 cm^{-1}) in Fig. 5. However, oxygen adatoms are involved in these reactions (29) and might either gain permanent residence at junction sites between metal atoms and TiO_x or actually promote surface restructuring of both the metal and the support catalyst components. Oxidative disruption of catalyst has been proposed for Ru/Al_2O_3 (26, 27). A pronounced spike in the spectrum at 2150 cm^{-1} (Fig. 4a) could be ascribed to CO ligated to oxidised Ru atoms (20, 26). Furthermore the absence of infrared bands at 1800–2000 cm^{-1} suggests a lack of exposed Rh^0 atoms. One reason could be that oxidative disruption had occurred, although coverage of Rh^0 sites by carbonaceous or hydrocarbonaceous adsorbate may also contribute to this result.

ACKNOWLEDGMENTS

We thank the Science and Engineering Research Council for a studentship, B.P. Chemicals (Hull) for collaboration through the CASE scheme, and Dr. R. D. Oades for helpful discussions.

REFERENCES

1. Morris, S. R., Moyes, R. B., Wells, P. B., and Whyman, R., *J. Catal.* **96,** 23 (1985).
2. Solymosi, F., Tombacz, I., and Kocsis, M., *J. Catal.* **75,** 78 (1982).
3. Tauster, S. J., Fung, S. C., and Garten, R. L., *J. Amer. Chem. Soc.* **100,** 170 (1978).
4. Levin, M. E., Salmeron, M., Bell, A. T., and Somorjai, G. A., *J. Chem. Soc. Faraday Trans. 1* **83,** 2061 (1987).
5. Belzunegui, J. P., Rojo, J. M., and Sanz, J., *J. Phys. Chem.* **95,** 3463 (1991).
6. Taniguchi, S., Mori, T., Mori, Y., Hattori, T., and Murakami, Y., *J. Catal.* **116,** 108 (1989).
7. Chudek, J. A., McQuire, M. W., McQuire, G. W., and Rochester, C. H., *J. Chem. Soc. Faraday Trans.* **91,** 3699 (1995).
8. Matani, A., and Chakrabarty, D. K., "Proceedings, 9th International Congress on Catalysis, Calgary, 1988," (M. J. Phillipps and M. Ternan, Eds), Vol. 2, p. 682. Chem. Institute of Canada, Ottawa, 1988.
9. Knifton, J. F., *J. Chem. Soc. Chem. Commun.,* 729 (1983).
10. Whyman, R., *J. Chem. Soc. Chem. Commun.,* 1439 (1983).
11. McQuire, M. W., and Rochester, C. H., *J. Catal.* **141,** 355 (1993).
12. McQuire, M. W., and Rochester, C. H., *J. Chem. Soc. Faraday Trans.* **89,** 1117 (1993).
13. Kellner, C. S., and Bell, A. T., *J. Catal.* **71,** 296 (1981).
14. Chudek, J. A., McQuire, M. W., and Rochester, C. H., *J. Catal.* **135,** 358 (1992).
15. Raskó, J., Bantovics, J., and Solymosi, F., *J. Catal.* **143,** 138 (1993).
16. Graham, J., Rochester, C. H., and Rudham, R., *J. Chem. Soc. Faraday Trans. 1* **77,** 1993 (1981).
17. Gonzalez, F., Munuera, G., and Prieto, J. A., *J. Chem. Soc. Faraday Trans. 1* **74,** 1517 (1978).
18. McQuire, M. W., Rochester, C. H., and Anderson, J. A., *J. Chem. Soc. Faraday Trans. 1* **88,** 879 (1992).
19. King, D. L., *Prepr. Am. Chem. Soc. Div. Pet. Chem.* **23,** 482 (1978).
20. Gupta, N. M., Kamble, V. S., Kartha, V. B., Iyer, R. M., Thampi, K. R., and Grätzel, M., *J. Catal.* **146,** 173 (1994).
21. Solymosi, F. and Knözinger, H., *J. Chem. Soc. Faraday Trans.* **86,** 389 (1990).
22. Solymosi, F., and Lancz, M., *J. Chem. Soc. Faraday Trans. 1* **82,** 883 (1986).
23. Pfnür, H., Menzel, M., Hoffmann, F. M., Ortega, A., and Bradshaw, A. M., *Surf. Sci.* **93,** 431 (1980).
24. Miura, H. M., McLaughlin, M. L., and Gonzalez, R. D., *J. Catal.* **79,** 227 (1983).
25. Buchanan, D. A., Hernandez, M. E., Solymosi, F., and White, J. M., *J. Catal.* **125,** 456 (1990).
26. Solymosi, F., and Raskó, J., *J. Catal.* **115,** 107 (1989).
27. Mizushima, T., Tohji, K., Udagawa, Y., and Ueno, A., *J. Phys. Chem.* **94,** 4980 (1990).
28. Dalla Betta, R. A., and Shelef, M., *J. Catal.* **48,** 111 (1977).
29. Low, G. G., and Bell, A. T., *J. Catal.* **57,** 397 (1979).
30. Duncan, T. M., Winslow, P., and Bell, A. T., *Chem. Phys. Lett.* **102,** 163 (1983).
31. Kellner, C. S., and Bell, A. T., *J. Catal.* **75,** 251 (1982).
32. Ekerdt, J. G., and Bell, A. T., *J. Catal.* **58,** 170 (1979).
33. Yamasaki, H., Kobori, Y., Naito, S., Onishi, T., and Tamaru, K., *J. Chem. Soc. Faraday Trans. 1* **77,** 2913 (1981).
34. Vannice, M. A., *J. Catal.* **37,** 462 (1975).
35. Apple, T. M., Gajardo, P., and Dybowski, C., *J. Catal.* **68,** 103 (1981).
36. McQuire, M. W., unpublished result.
37. Kelley, R. D., and Goodman, D. W., *Surface Sci.* **123,** L743 (1982).